Tubulin cofactor A gene silencing in mammalian cells induces changes in microtubule cytoskeleton, cell cycle arrest and cell death

Sofia Nolasco[a], Javier Bellido[b], João Gonçalves[a], Juan Carlos Zabala[b], Helena Soares[a,c,*]

[a] *Instituto Gulbenkian de Ciência, Apartado 14, 2781-901 Oeiras, Portugal*
[b] *Departamento de Biologia Molecular-Unidad asociada al Centro de Investigaciones Biologicas (CSIC), Universidad de Cantabria, 39011 Santander, Spain*
[c] *Escola Superior de Tecnologia da Saúde de Lisboa, 1990-096 Lisboa, Portugal*

Received 9 March 2005; revised 26 April 2005; accepted 4 May 2005

Available online 4 June 2005

Edited by Michael R. Bubb

Abstract Microtubules are polymers of α/β-tubulin participating in essential cell functions. A multistep process involving distinct molecular chaperones and cofactors produces new tubulin heterodimers competent to polymerise. In vitro cofactor A (TBCA) interacts with β-tubulin in a quasi-native state behaving as a molecular chaperone. We have used siRNA to silence TBCA expression in HeLa and MCF-7 mammalian cell lines. TBCA is essential for cell viability and its knockdown produces a decrease in the amount of soluble tubulin, modifications in microtubules and G1 cell cycle arrest. In MCF-7 cells, cell death was preceded by a change in cell shape resembling differentiation.

Keywords: β-Tubulin cofactor A (TBCA); Molecular chaperone; Folding; Apoptosis; Microtubules

1. Introduction

Microtubules (Mts) are polarized polymers of α/β-tubulin heterodimers participating in a wide range of both essential and specialized cell functions [1,2]. How Mts accomplish this variety of functions is far from being completely understood. These functions are controlled by two major protein groups: (1) Mt associated proteins (MAPs) that modulate their dynamic instability, or regulate transport processes and/or their organization by connecting them to cellular structures or other cytoskeleton filaments [3,4]; (2) molecular chaperones and tubulin cofactors coordinating Mt biogenesis and recycling of tubulin heterodimers [5].

The generation of new tubulin heterodimers is a multi-step process involving several protein tubulin cofactors (TBCs). Nascent α- and β-tubulin chains first interact with prefoldin that delivers them to the cytosolic chaperonin CCT (Cytosolic-Chaperonin-containing-TCP1). Afterwards, as suggested by in vitro folding assays tubulins follow two different folding pathways; α-tubulin is captured by cofactor B (TBCB), while β-tubulin by cofactor A (TBCA) [6,7]. Then cofactors E (TBCE) and D (TBCD) will capture α- and β-tubulin, respectively. The two pathways converge and α-tubulin, β-tubulin, TBCE and TBCD form a super-complex. Cofactor C (TBCC) would interact with this complex and upon GTP hydrolysis assembly competent α/β-tubulin heterodimers are released [8]. The small G-protein Arl2 appears to play a regulatory role in this pathway, binding to TBCD and sequestering it [9]. In *Saccharomyces cerevisiae* TBCs genes were identified in mutant screens for cells that were compromised in Mts-dependent functions. Yeast TBCs genes are not essential, but their mutations confer an increased frequency of chromosome loss, hypersensitivity to Mt-disrupting drugs and show genetic interactions with tubulin mutations [10,11].

Rbl2p, the TBCA yeast orthologue, has about 30% identity to mammalian TBCA and was identified as a protein capable of rescuing cells from lethal β-tubulin overexpression, serving as a reservoir of excess β-tubulin [10]. *RBL2*$^{(A)}$ is not an essential gene in yeast but is required for normal meiosis [10]. In the fission yeast, *Schizosaccharomyces pombe*, TBCs genes are essential except the TBCA orthologue gene, *alp31*$^{+}$ [12]. Alp31$^{(A)}$ has about 30% identity to mammalian TBCA and plays an important role in the maintenance of Mts integrity and the determination of the cell polarity [12]. This family of proteins appears to be functionally compatible, since murine TBCA can complement the Rbl2p^{A} function in *S. cerevisiae* [10] and Alp31$^{(A)}$ in *S. pombe* [12]. TBCA is not required for in vitro β-tubulin folding [13] consistent with the non-essential behaviour of Rbl2p$^{(A)}$ and Alp31$^{(A)}$ proteins [10,12]. In vitro experiments show that TBCA plays a dual role inside of the cell: on one hand, enhancing the dimerization rate of β-tubulin, and on the other hand, serving as a reservoir of excess β-tubulin [14]. Overexpression experiments of TBCA and Rbl2p$^{(A)}$ have failed to demonstrate a clear phenotype [14], in contrast, overproduction of Alp31$^{(A)}$ results in the disappearance of intact Mts structures associated with cell polarity defects [12].

TBCA expression was analysed in different murine tissues. TBCA is more abundantly expressed in testis and is progressively upregulated from the onset of meiosis through spermiogenesis, being more abundant in differentiating spermatids. TBCA expression seems to be associated to Mt cytoskeleton changes and with β-tubulin processing through spermatogenesis rather than meiosis [15].

Morphology-based mutant screens have identified TBCs as essential players in plant morphogenesis [16]. The *Arabidopsis PILZ* group genes encode orthologues of mammalian TBCC, TBCD, and TBCE, and the associated small G-protein Arl2. Another gene with related mutant phenotype, *KIESEL*,

*Corresponding author. Fax: +351 21 4407970.
E-mail address: msoares@igc.gulbenkian.pt (H. Soares).

0014-5793/$30.00
doi:10.1016/j.febslet.2005.05.022

encodes the TBCA orthologue. Different studies carried out in *Arabidopsis* have given results resembling the mammalian in vitro tubulin folding pathway model [16]. In contrast with both yeast strains, in *Arabidopsis kis*$^{(A)}$ mutants result in embryonic lethality with less severe phenotype than *pilz*$^{(C/D/E/Arl2)}$ group mutants [16,17].

In vivo requirements of mammalian TBCs are still unknown due to lack of loss-of-function studies. In this work, we show that mammalian TBCA is essential for cell viability and the results are discussed in view of soluble tubulin levels and Mt cytoskeleton alterations and how these may lead to cell death.

2. Materials and methods

2.1. Cell culture

Tumour cell lines HeLa and MCF-7 were cultured in a 5% CO_2 humidified atmosphere at 37 °C as exponentially growing sub-confluent monolayers in Dulbecco's modified Eagle's medium (DMEM) with glutamax (Invitrogen), supplemented with 10% fetal calf serum (Invitrogen) and non-essential aminoacids (Invitrogen).

2.2. siRNA design and transfection

TBCA siRNA was designed according to criteria outlined elsewhere [18]. The target sequence is located in the C-terminal coding region, between nucleotide positions 334 and 352 (^{334}AGAAGCACGTTTAGTACTG^{352}) relative to the first nucleotide of the start codon of TBCA gene [NM_004607]. TBCA siRNA was 21 nucleotides long containing symmetric 3′ overhangs of two deoxythymidines. The non-target, fluorescent, stable control siRNA with RISC-free modification, siGlo RISC-free siRNA, was used as a negative control. Both siRNAs were synthesized by Dharmacon Research, Inc.

Transfections were performed with oligofectamine (Invitrogen) as specified by the manufacturer. At 18 h prior to transfection, 2.5×10^4 cells were seeded per well for a 24-well plate or 1×10^5 cells were seeded per well for a 6-well plate. The final concentrations of siRNAs in the culture media were 100 nM. For transfection, siRNAs and oligofectamine were diluted in Opti-MEM I (Invitrogen).

The dependence of the blebbing phenotype on caspase activities was investigated in TBCA siRNA transfected HeLa cells using the broad spectrum caspase inhibitor, Z-VAD-FMK (Bachem). Cells were treated with 100 μM of Z-VAD-FMK for 1 h before transfection and the inhibitor was maintained during the whole period of transfection studied.

2.3. RNA extraction and RT-PCRs

Total RNA was extracted using RNeasy micro-kit (Qiagen), according to the manufacturer's protocol. The RNA was treated with DNase I (Amersham–Pharmacia Biotech) and reverse transcribed using SuperScript II (Invitrogen) and oligo(dT)$_{12–18}$ primer (Amersham–Pharmacia Biotech). The RT-PCR procedure was adapted from Meadus [19]. The amount of cDNA in each sample was first normalized after non-saturing PCR for HPRT (hypoxanthine guanine phosphoribosyl transferase 1-standard internal control) transcripts. 25 μl reaction mixture contained 1.5 mM $MgCl_2$, 0.2 mM dNTPs, 30 pmol of sense primer (Table 1), 30 pmol of antisense primer (Table 1) and 1 U *Taq* DNA polymerase (Invitrogen) in the manufacturer's buffer. PCR consisted of 5 min at 94 °C followed by 28 cycles of 30 s at 94 °C, 30 s at 53 °C, and 1 min at 72 °C, and the reaction was stopped at 72 °C for 10 min. All PCRs were performed on a Mastercycler Personal (Eppendorf). After separation on 2% agarose (SeaKem) gels, the images were acquired and digitalized with an Eagle Eye II still video system (Stratagene). The amount of PCR DNA products was quantified using the ImageJ software.

2.4. Protein extraction and Western blot analysis

For protein extraction cells were rinsed with PBS, and then lysed in buffer containing 100 mM MES, pH 6.7 (Sigma); 1 mM $MgCl_2$ (Merck); 1 mM EGTA (Sigma); 0.1 mM GTP (Sigma); 0.1% NP-40 (Sigma); 0.2 mM DTT (Sigma) and 0.1 mM PMSF (Sigma), containing a protease inhibitors cocktail. Cellular lysates were removed from culture plates by scraping and then centrifuged at $14000 \times g$ for 30 min at 4 °C and the supernatants were recovered (post-mitochondrial fraction). Total protein extracts were prepared using the same lysing buffer after the addition of 7.5% of 2-mercaptoethanol (Sigma). Equal amounts of post-mitochondrial protein extracts, obtained from the same number of non-transfected cells and cells transfected with TBCA siRNA and with non-target siRNA, were separated on a 16.5% (w/v) Tricine–SDS–PAGE [20]. Similarly, equal amounts of total protein extracts, prepared from the same number of non-transfected cells and cells transfected with TBCA siRNA, were analysed in 10% (w/v) SDS–PAGE. Westerns blots were performed accordingly to [21] using the rabbit polyclonal sera against TBCA (1:5000) [22], the mouse monoclonal antibody against α-tubulin (1:1000) (clone DM1A, Sigma), the mouse monoclonal antibody against β-tubulin (1:1000) (clone TUB 2.1, Sigma), the rabbit polyclonal sera against Hsp70 (1:5000) (Stressgen) and the rabbit anti-PARP polyclonal antibody (1:3000) (Stressgen). Secondary antibodies against mouse (Jackson ImmunoResearch) and rabbit (Zymed) were used at 1:4000 and 1:2000, respectively. The immunostaining was carried out using the ECL technique (Amersham–Pharmacia Biotech). The molecular mass markers used were purchased from Amersham–Pharmacia Biotech.

Table 1
Primer sequences specific for human TBCA, β-tubulin and HPRT used in PCRs

Genes	Sequences
TBCA*	5′-GTGAAGCGGTTGGTCAAAG-3′ 5′-GCAGTGGTCAAAAATAATGG-3′
β-Tubulin*	5′-GGGGCAGGTAACAACTGGG-3′ 5′-GAGGTCAGCATTGAGCTGG-3′
HPRT*	5′-GGCGTCGTGATTAGTGATG-3′ 5′-CATTACAATAGCTCTTCAGTC-3′

*Accession number TBCA (NM_004607); β-tubulin (NM_178014) and HRPT (NM_000194).

2.5. Transmitted light microscopy

Living HeLa cells were grown in a culture DMEM medium without phenol red (Invitrogen) and were directly observed by inverted transmitted light microscope (Leica Inverted CCD microscope). The image acquisition was carried out using a cooled CCD camera and MetaMorph Imaging Software (Universal Imaging Corporation). The image processing was performed using ImageJ Software.

2.6. Fluorescence microscopy

Cells processed for fluorescence microscopy were washed twice with PBS (Invitrogen) and then fixed in 3.7% (w/v) paraformaldehyde (Merck) in PBS for 10 min at room temperature. Then they were washed twice with PBS for 5 min and permeabilized during 2 min using 0.1% (v/v) Triton X-100 (Sigma) in PBS. After rinsing twice for 5 min in PBS and once in PBS-0.1% (v/v) Tween (Merck) cells were blocked in 3% (w/v) BSA (Calbiochem) for 15 min. Next, cells were simultaneous incubated with phalloidin (phalloidin–Tetramethylrhodamine B isothiocyanate) (1:200) (Sigma) and with the mouse monoclonal α-tubulin antibody (clone DM1A) (1:200) (Sigma) in the same solution for 1 h. Samples were washed twice in PBS for 5 min and once in PBS-0.1% (v/v) Tween. Secondary antibody Alexa Fluor 488-conjugated goat anti-mouse IgG (1:500) (Molecular Probes) was incubated for 1 h in the same solution. The preparations were washed twice in PBS for 5 min and once in PBS-0.1% (v/v) Tween. DNA was stained with DAPI (1 μg/μl, Sigma) in PBS for 1 min. The preparations were washed in PBS and mounted in MOWIOL 4-88 (Calbiochem) mounting medium supplemented with 2.5% (w/v) DABCO (Sigma).

Cells were examined with a fluorescence microscope (Leica DMRA2) and image acquisition was performed with a cooled CCD camera and MetaMorph Imaging Software (Universal Imaging Corporation). The image processing was carried out with ImageJ Software.

2.7. Cell cycle analysis by flow cytometry

For the determination of cell cycle distribution, cells were harvested, washed with PBS and fixed with ice-cold 70% ethanol in PBS. After that the cells were incubated in PBS with 0.1% (v/v) Triton X-100 (Sigma) and 5 μg/ml of RNase (Roche) for 30 min at room temperature. 50 ng/ml of propidium iodide (Sigma) in PBS-0.1% (v/v) Triton X-100 was added to the cells for 5 min in the dark at room temperature. Subsequently, cells were washed in PBS and the cell cycle distribution was analysed on FACSCalibur (Becton–Dickinson, Mountain View, CA) using Cell Quest™ software.

3. Results

3.1. TBCA knockdown by RNAi leads to cell death in HeLa cells

There are only a few studies reporting the role of TBCA in vivo [for review 14, 16, 17]. Therefore, not much is known about its role especially in multicellular organisms that show larger tubulin gene families and express distinct tubulin isotypes and show more complex Mt structures. Consequently, we have investigated the phenotypic effects of TBCA knockdown in mammalian cell lines by selectively silencing the expression of the TBCA gene protein using RNAi technology (see Section 2).

The efficiency of siRNA transfection in HeLa cells was estimated using a non-target, non-functional fluorescent labeled siRNA. The fluorescence was correlated with the functional siRNA uptake (data not shown). Using this control we observed a transfection efficiency of about 90–100%. The non-target siRNA was also used to check for general non-specific effects associated with siRNA delivery and to confirm the sequence specificity of the silencing effect (negative control).

We tested the efficacy of the TBCA siRNA silencing by analysing the TBCA mRNA and TBCA protein levels (Fig. 1A and B). Total RNA was extracted from HeLa cells transfected for 48 h with non-target siRNA and with TBCA siRNA and then analysed by RT-PCR. Semi-quantitative RT-PCR analysis showed a decrease of steady-state levels of TBCA mRNA in TBCA siRNA transfected cells in comparison with those found in cells transfected with non-target siRNA. This indicates that TBCA siRNA promotes the silencing of TBCA gene (Fig. 1A). The steady-state levels of β-tubulin and HRPT mRNAs did not significantly change in TBCA siRNA transfected cells.

Equal amounts of post-mitochondrial protein extracts of HeLa cells not transfected and transfected with TBCA siRNA for 24, 48 and 72 h were analysed by Western blot using a set of antibodies against TBCA, α- and β-tubulin and Hsp70 (Fig. 1B). Similarly, cells transfected with non-target siRNA for 48 h were also analysed. A decrease in the steady-state levels of TBCA were detected in TBCA knockdown transfected cells after 24 h post-transfection. This decrease was also accompanied by a decrease of α- and β-tubulin amounts, whereas there were no significant changes in steady state levels of Hsp70. In both cases the low levels were maintained until 72 h post-transfection (Fig. 1B).

After transfection of HeLa cells with TBCA siRNA we investigated the effects of TBCA silencing in cell survival by studying the cells growth and morphology using transmitted light microscopy (Fig. 1C). At 24 h post-transfection all cell samples transfected either with non-target siRNA or TBCA siRNA present a percentage of dead cells (round detached cells) similar to that observed for non-transfected cells. After 48 and 72 h of transfection with non-target siRNA cells were still proliferating originating small islands of growing cells with no changes in their normal shape (Fig. 1C). In contrast, TBCA siRNA transfected cells exhibited a progressive increase of cell death, visible by the increasing number of small round detached cells (Fig. 1C). After 72 h of TBCA siRNA transfection there were practically no living cells (results not shown).

Taken together our results support that TBCA is an essential gene for human cells since its silencing by specific TBCA siRNA leads to cell death between 48 and 72 h after transfection.

3.2. Alterations of microtubule and actin cytoskeleton associated with TBCA siRNA transfection in HeLa cells

The fact that TBCA is described as being able to enhance β-tubulin dimerization and to serve as a reservoir of excess of tubulin [14], lead us to investigate if HeLa cells transfected with TBCA siRNA would exhibit defects in the cytoskeleton that correlate with previously observed cell death. Therefore, we studied the Mt and actin cytoskeletons in HeLa cells transfected with TBCA siRNA for 24 h using fluorescence microscopy. Mt cytoskeleton was visualized using an antibody against α-tubulin whereas actin cytoskeleton was stained with phalloidin. Fig. 2A reveals that the Mt cytoskeleton of TBCA siRNA transfected HeLa cells show only subtle alterations when compared to that of non-target siRNA transfected cells or cells not transfected. TBCA siRNA transfected cells are reduced in size, which makes the analysis of the Mt cytoskeleton difficult. However, we observed a decrease in Mt amount simultaneous with a diffuse labelling in the periphery of the cell resembling a partial Mt depolymerization (Fig. 2A, see arrows). These cells also showed a significant decrease in the number of mitotic spindles. Interestingly, the actin cytoskeleton was undoubtedly altered, since a clear marginal membrane blebbing is observed (Fig. 2). This phenotype was a representative feature of the HeLa cells transfected with TBCA siRNA because there is a threefold increase of the blebbing phenotype in HeLa cells transfected with TBCA siRNA (Fig. 2B). The blebbing phenotype caused by TBCA silencing could be related with an apoptotic event triggered by the alterations detected in Mt and actin cytoskeleton. Indeed, the blebbing phenotype can be induced by local actin depolymerization [23,24] or cross-linking of actin filaments [24,25] and by disassembly of Mts [26,27]. Recently, the marginal blebbing of TNF-induced apoptosis was also described like an early microfilament-dependent apoptotic event [28].

3.3. TBCA knockdown in MCF-7 cells

To investigate if the blebbing phenotype observed in TBCA depleted HeLa cells was a consequence of an apoptotic event related to caspase-3 activation, we transfected MCF-7 cells, a caspase-3 defective cell line, with the same TBCA siRNA [29]. Transfection efficiency and efficacy of TBCA siRNA were performed by experiments similar to those described for HeLa cells. Total RNA was extracted from MCF-7 cells transfected for 72 h with non-target siRNA and with TBCA siRNA. Semi-quantitative RT-PCR analysis showed a decrease of steady-state levels of TBCA mRNA in TBCA siRNA transfected cells, whereas the steady-state levels of HPRT and β-tubulin mRNAs did not significantly change (Fig. 3A).

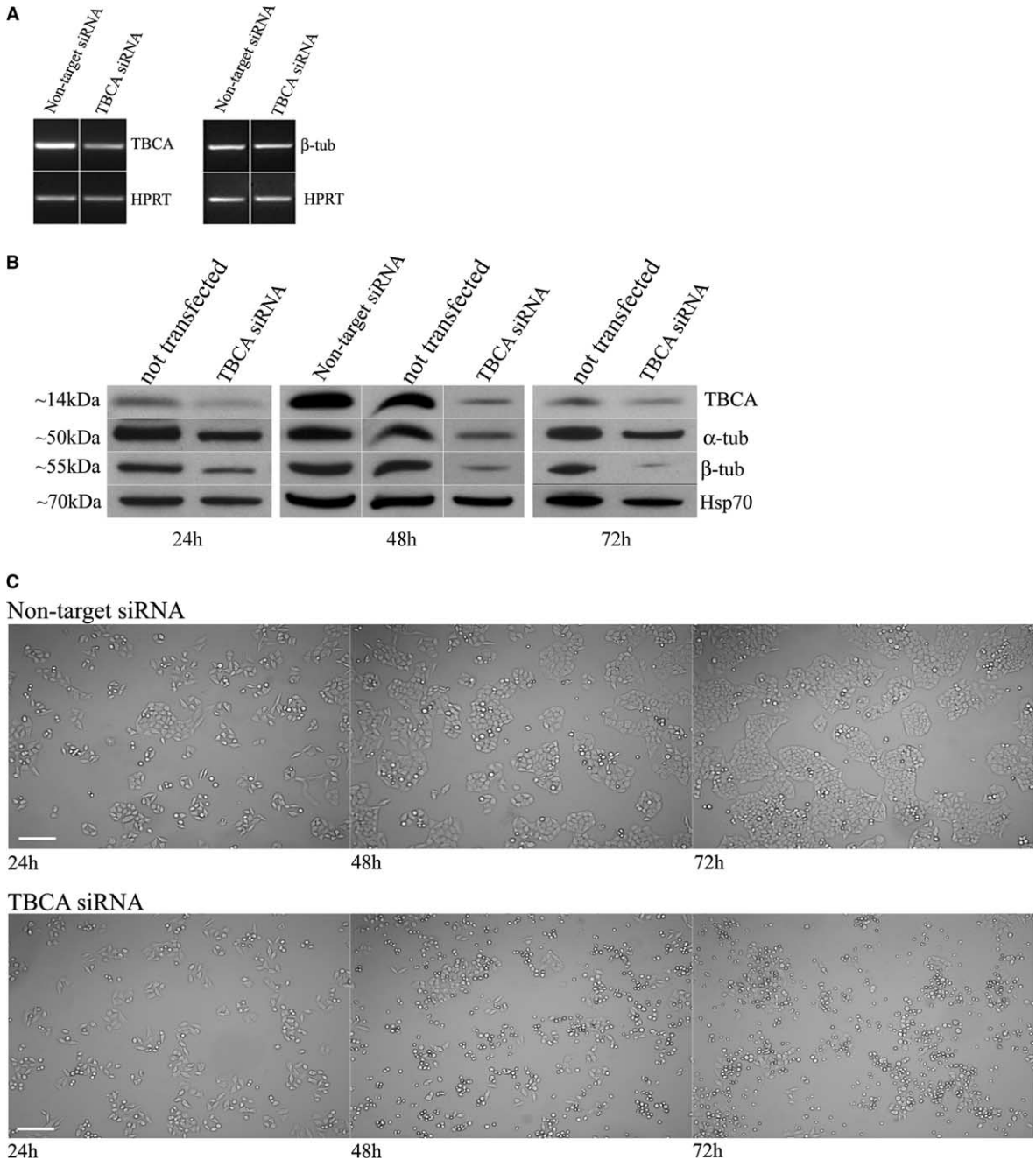

Fig. 1. TBCA knockdown by RNAi leads to cell death in HeLa cells. After 48 h of transfection total RNA was prepared from HeLa cells transfected with non-target siRNA and TBCA siRNAs (A). Similarly, post-mitochondrial protein extracts were prepared from HeLa cells not transfected and transfected for 24, 48 and 72 h with TBCA siRNAs (B). Post-mitochondrial protein extracts were also prepared from HeLa cells transfected with non-target siRNA for 48 h (B). (A) Semi-quantitative RT-PCR analysis showed a decrease in the steady-state levels of TBCA mRNA in TBCA siRNA transfected cells in comparison to those in cells transfected with non-target siRNA. The steady-state levels of HPRT and β-tubulin mRNAs remain constant in these cells. (B) For each time studied, equal amount of post-mitochondrial protein extracts were analysed by 16.5% (w/v) Tricine–SDS–PAGE followed by Western blot with antibodies directed to TBCA, α-, β-tubulin and Hsp70. Cells transfected for 24 h with TBCA siRNAs showed a decrease in steady-state levels of TBCA, as well as in the levels of α- and β-tubulin when compared with those in control cells. The low levels of these proteins are maintained until 72 h post-transfection. Hsp70 protein levels were used as a loading control. The approximate molecular mass of the proteins are indicated at the left side of the panels. (C) After 24, 48 and 72 h of transfection with non-target and with TBCA siRNAs, HeLa cells were observed by transmitted light microscopy. Cell death increase was observed upon silencing of TBCA in proliferating HeLa cells. Scale bar ~150 μm.

Post-mitochondrial protein extracts of MCF-7 cells were prepared from not transfected and transfected cells after 24, 48, 72 and 96 h with TBCA siRNA and then analysed by Western blot using antibodies against TBCA, tubulin and Hsp70 (Fig. 3B). Transfected cells with non-target siRNA for 72 h were also analysed. In contrary to HeLa cells, a decrease in the steady-state amount of TBCA protein was only detected in cells transfected with TBCA siRNA after 48 h. However,

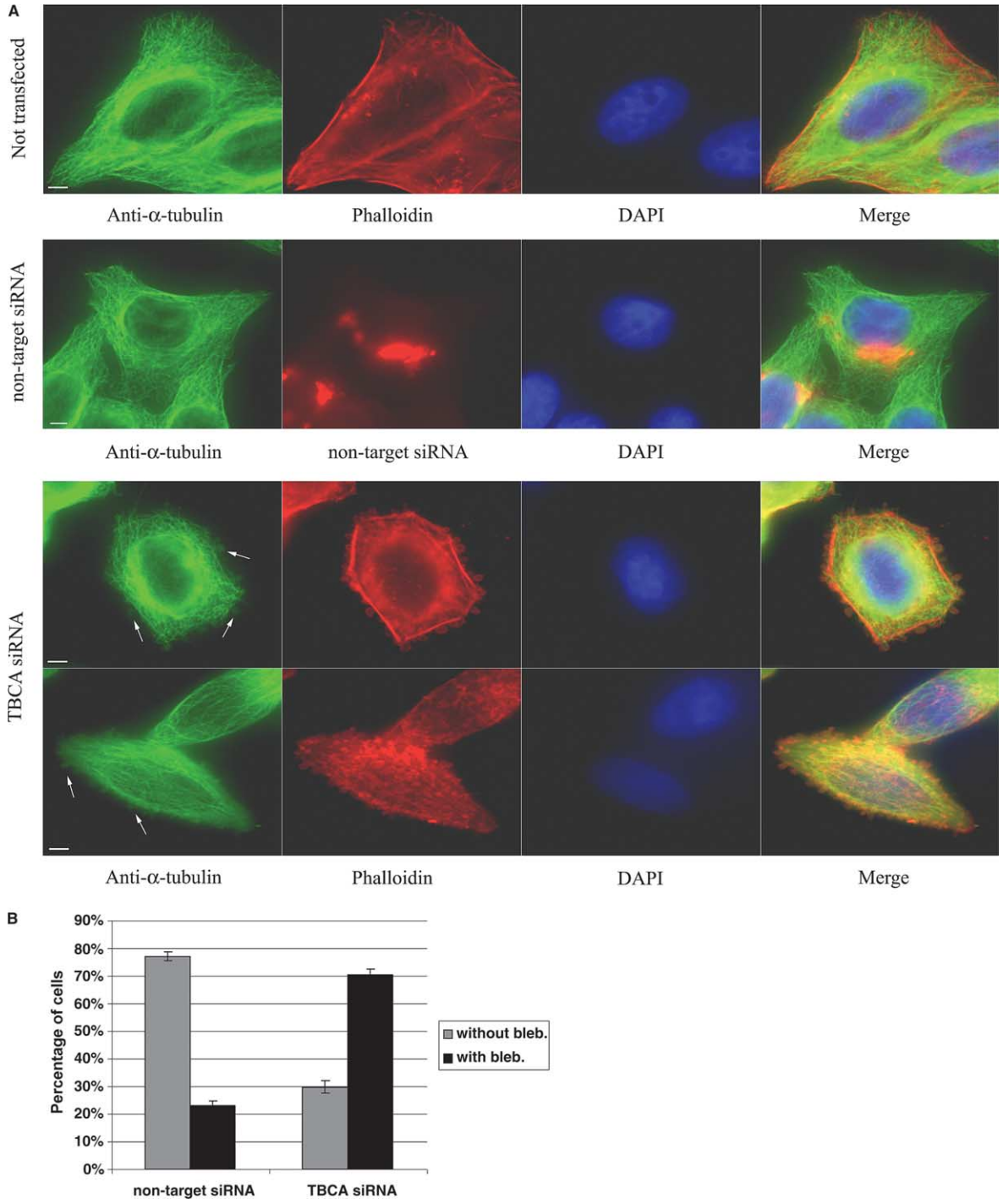

Fig. 2. Phenotype analysis of HeLa cells 24 h after TBCA siRNA transfection, assessed by indirect immunolocalization of tubulin and staining of actin. (A) After 24 h of siRNA transfection, HeLa cells were processed for immunofluorescence microscopy using the antibody directed to α-tubulin, the phalloidin stain as a fluorescent probe for F-actin and DAPI as a nucleic acid stain. Merged images are shown at right edge panels. As a control we used the non-target siRNA. Representative images show that TBCA siRNA transfected cells have subtle changes in Mt cytoskeleton showing at periphery a diffuse staining resembling partial depolymerization (see arrows). Actin cytoskeleton presents a clear marginal blebbing. Scale bar = 4 μm. (B) The number of cells with and without marginal blebbing was determined in HeLa cells transfected with non-target siRNA and with TBCA siRNA. Graphic bars show mean values of two independent experiments. In each experiment, ~1700 cells were counted. An increase of the blebbing phenotype associated with TBCA siRNA transfection in HeLa cells is clearly visible.

we did not observe a decrease in steady-state levels of α- and β-tubulin in TBCA siRNA transfected MCF-7 cells until 96 h post-transfection. During the time course studied the steady-state levels of Hsp70 continue almost unaltered (Fig. 3B).

The cytoskeleton phenotype of TBCA siRNA MCF-7 transfected cells for 48 h was also investigated as described for HeLa cells (Fig. 3C; I–IV). We chose cells transfected with TBCA siRNA after 48 h because this corresponds to the time

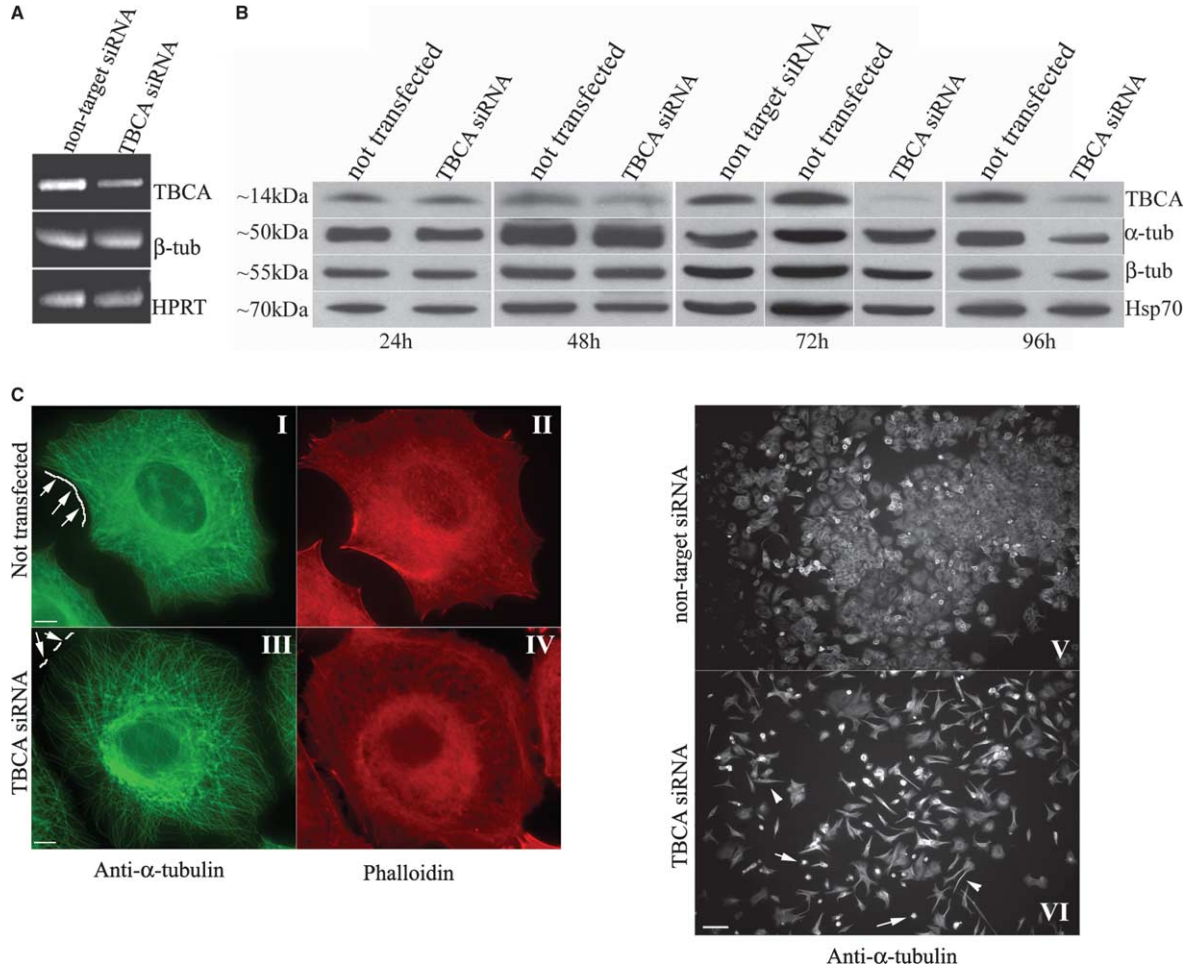

Fig. 3. TBCA silencing in MCF-7 cells. Phenotype analysis by indirect immunolocalization of tubulin and staining of actin. Total RNA was obtained from MCF-7 cells 72 h post-transfection with non-target siRNA and TBCA siRNAs (A). Post-mitochondrial protein extracts were prepared from MCF-7 cells not transfected and transfected for 24, 48, 72 and 96 h with TBCA siRNAs (B). Also, post-mitochondrial protein extracts were also prepared from MCF-7 cells transfected with non-target siRNA for 72 h (B). (A) Semi-quantitative RT-PCR analysis showed a decrease of steady-state levels of TBCA mRNAs in TBCA siRNA transfected cells compared to those found in cells transfected with non-target siRNA. The steady-state levels of HPRT and β-tubulin mRNAs are constant in these cells. (B) For each time studied, equal amount of post-mitochondrial protein extracts were separated by 16.5% (w/v) Tricine–SDS–PAGE and analysed by Western blot using antibodies against TBCA, α-, β-tubulin and Hsp70 proteins. Cells transfected with TBCA siRNAs showed a decrease in steady-state levels of TBCA protein at 48 h after transfection, whereas steady-state levels of α- and β-tubulin proteins only decrease after 96 h post-transfection. Hsp70 protein levels were used as a loading control. The approximate molecular mass of the proteins are indicated at the left side of the panels. (C) After 48 and 96 h of siRNA transfection, MCF-7 cells were processed for immunofluorescence microscopy using the antibody directed to α-tubulin (I, III, V and VI) and the phalloidin stain as a fluorescent probe for F-actin (II and IV). As a control we used the not transfected cells. The images shown are representative of at least four independent experiments. Comparison with cells not transfected (I and II) and transfected for 48 h with TBCA siRNA (III and IV) shows that transfected cells have a slight decrease in Mts amount (see arrows) and marginal blebbing was not observed. Scale bar = 6 μm (for I–IV). After 96 h of transfection with TBCA, siRNA cells were dying (VI, see arrows) or became more ''spindle-like'' (VI, see arrow heads) when compared with those transfected with non-target siRNA (V). Scale bar = 90 μm (for V and VI).

where a clear decrease in TBCA was observed. In comparison with control cells, MCF-7 cells transfected with TBCA siRNA seem to have a lower amount of Mts (Fig. 3C; I and III). A careful analysis of a considerable number of MCF-7 cells transfected with TBCA siRNA (>1000 cells from three independent experiments) showed that this was a subtle feature in most of them. However, in these cells the absence of mitotic spindles was clearly observable, as well as the absence of blebbing phenotype. Moreover, until 72 h of post-transfection of MCF-7 cells, the cell death phenotype was not observed. At 96 h after transfection, we detected an increase in MCF-7 dying cells (rounded up cells) and in spindle-shaped cells, resembling differentiated cells, a cell shape modification that probably precedes cell death (Fig. 3C compare panel V with panel VI).

The phenotype differences found between HeLa and MCF-7 cells may be related to the fact that the tubulin levels did not decrease in MCF-7 cells until 96 h after TBCA siRNA transfection. However, we can not exclude the hypothesis that the absence of the blebbing phenotype in these cells may be related with the lack of an active capase-3.

To discriminate between these two hypotheses, we have investigated if caspase activity was associated with the blebbing phenotype presented by HeLa cells after TBCA knockdown. For this purpose we treated this cell line, prior to TBCA siRNA transfection, with Z-VAD-FMK an irreversible

caspase inhibitor. We observed that caspase inhibition did not abolish or reduce the blebbing phenotype of HeLa cells transfected with TBCA siRNA (results not shown). However, we detected a delay in cell death rate during the transfection time tested (24–72 h) (Fig. 4A). This observation indicates that Z-VAD-FMK is active and caspases are involved in cell death. Additionally, in all the experiments the caspase inhibition by Z-VAD-FMK was assessed by performing Western blot analysis of total protein extracts prepared from cells transfected with TBCA siRNA in the presence or absence of the caspase activity inhibitor Z-VAD-FMK using the antibody against the Poly (ADP-ribose) polymerase (PARP). PARP is a nuclear protein involved in DNA repair and an early marker for apoptosis. Upon induction of apoptosis PARP is cleaved by caspase-3 and caspase-7 [30]. As can be seen from Fig. 4B, in HeLa cells only transfected with TBCA siRNA the non-cleaved PARP protein levels are lower (~50%) than those found in HeLa cells transfected with TBCA siRNA and treated with Z-VAD-FMK. This result indicates that in the presence of Z-VAD-FMK PARP is not cleaved. These experiments show that in HeLa cells the blebbing phenotype could not be explained by the presence of an active caspase-3 or other caspases activity.

3.4. TBCA knockdown results in caspase-7 activation but cell death occurs essentially by secondary necrosis

The obtained results using the caspase inhibitor Z-VAD-FMK indicated that TBCA siRNA transfected cells were dying

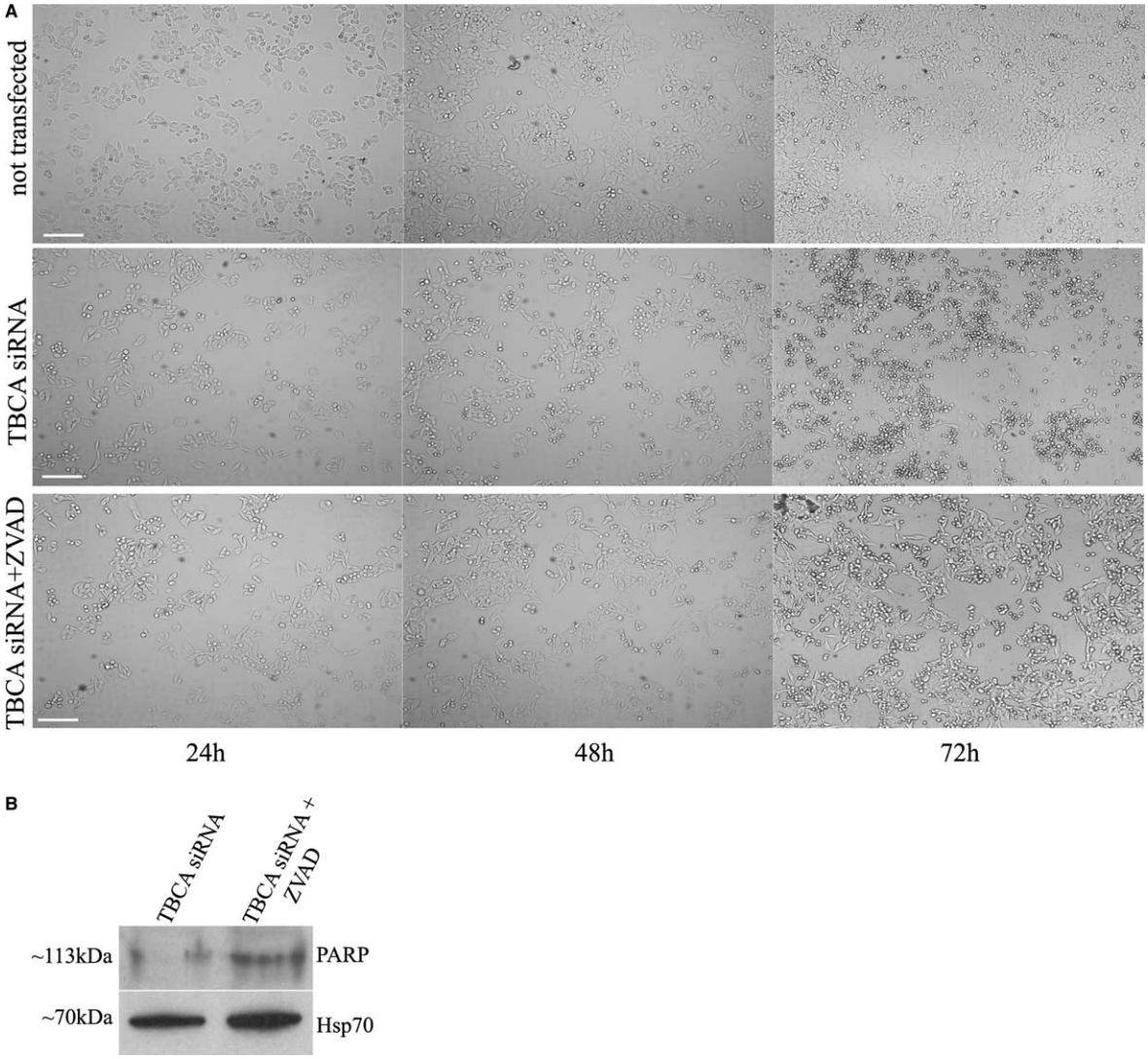

Fig. 4. Influence of the caspase inhibitor Z-VAD-FMK in the TBCA knockdown phenotype in HeLa cells. HeLa cells not transfected or transfected for 24, 48 and 72 h with TBCA siRNAs, in the presence or absence of the caspase activity inhibitor Z-VAD-FMK, were observed by transmitted light microscopy (A). In the presence of Z-VAD-FMK a decrease in cell death was observed upon silencing of TBCA in proliferating HeLa cells. Scale bar ~150 μm. To test the inhibitor activity of Z-VAD-FMK equal amounts of total protein extracts were prepared from HeLa cells transfected for 24 h with TBCA siRNA, in presence and absence of the inhibitor and analysed by 10% (w/v) SDS–PAGE, and then Western blotted using the antibody against the nuclear protein PARP, an early marker for apoptosis (B). In HeLa cells transfected with TBCA siRNA and treated with Z-VAD-FMK the non-cleaved PARP protein levels are higher than those found in HeLa cells only transfected with TBCA siRNA, indicating that PARP is not being cleaved. HSP 70 protein levels were used as a loading control. The approximate molecular mass of the proteins are indicated at the left side of the panel.

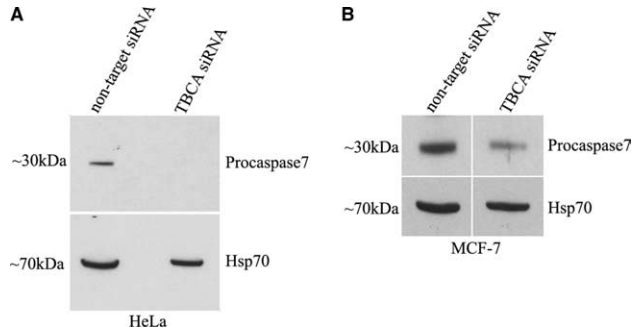

Fig. 5. TBCA knockdown by RNAi induces caspase-7 activation. Equal amount of post-mitochondrial protein extracts from HeLa and MCF-7 cells transfected with TBCA and with non-target siRNAs for 48 h (A) and for 72 h (B), respectively, were analysed by 16.5% (w/v) Tricine–SDS–PAGE followed by Western blot using antibodies specific against procaspase-7 and Hsp70. Cells transfected with TBCA siRNAs showed a decrease in steady-state levels of procaspase-7, indicating an activation of caspase-7. Hsp70 protein levels were used as a loading control. The approximate molecular mass of the proteins are indicated at the left side of the panels.

by apoptotic pathways. To confirm this hypothesis we decided to check the caspase-7 activation. Post-mitochondrial proteins extracts of cells transfected with TBCA and non-target siRNAs, after 48 h for HeLa cells (Fig. 5A) and after 72 h for MCF-7 cells (Fig. 5B), were prepared and then analysed by Western blot. Cells transfected with TBCA siRNAs showed a decrease in the steady-state levels of procaspase-7, indicating its activation. However, the simultaneous Annexin-V-FLUO and PI staining showed that the majority of Annexin-V stained population of cells were also PI positive (results not shown). Although, the TBCA knockdown causes cleavage of PARP protein and also the activation of caspase-7, the observed cell death seems to occur mainly by necrosis/late apoptosis (secondary necrosis) [31].

3.5. TBCA knockdown in HeLa and MCF-7 cells results in G1 cell cycle arrest

The observation that MCF-7 cells, 48 and 72 h after transfection with TBCA siRNA, did not possess visible mitotic spindles prompted us to analyse the cell cycle progression in these and in HeLa cells by flow cytometry (FACS analysis). HeLa and MCF-7 cells not transfected and transfected with TBCA siRNA for 24 and for 72 h, respectively, were fixed and stained with propidium iodide. For these cells, the cell cycle distribution was established by FACS analysis based on DNA content. This analysis indicates a G1 cell cycle arrest in HeLa and MCF-7 cells transfected with TBCA siRNA (see profiles of Fig. 6A and B). FACS analysis also confirmed the cell shape alteration detected in MCF-7 cells, showing that these cells have an increased width (data not shown).

4. Discussion

Mts assembly is dependent on a tubulin heterodimers pool competent to polymerize. The production of native tubulin heterodimers requires a complex folding pathway involving distinct molecular chaperones (prefoldin and cytosolic chaperonin CCT) and cofactors (TBCA-TBCE). We have investigated the effects of TBCA knockdown in mammalian cell lines, HeLa and MCF-7, by selective TBCA silencing using siRNA. In both cell lines we observed the occurrence of cell death, and therefore TBCA is an essential protein for human cells. Until now, there were no studies of tubulin cofactors loss-of-function in mammalian cells. It is most likely that in vitro folding assays, where TBCA is not necessary for β-tubulin folding [13], may not reflect the in vivo requirements. If the most important activity of TBCA is to avoid β-tubulin unfolding to prevent aggregation, a dispensable TBCA function in vitro in the presence of the other cofactors will be expected [13]. This may contrast with the in vivo situation where chaperones are required to prevent misfolding until the substrate enters into the next folding complex.

We have investigated if mammalian cell death caused by TBCA knockdown was correlated with Mt and actin cytoskeleton alterations. Our results demonstrated that TBCA siRNA transfected HeLa cells have Mt cytoskeleton disturbed (Fig. 2). This may reflect the decrease of β-tubulin steady-state levels detected in this cell line upon transfection that are accompa-

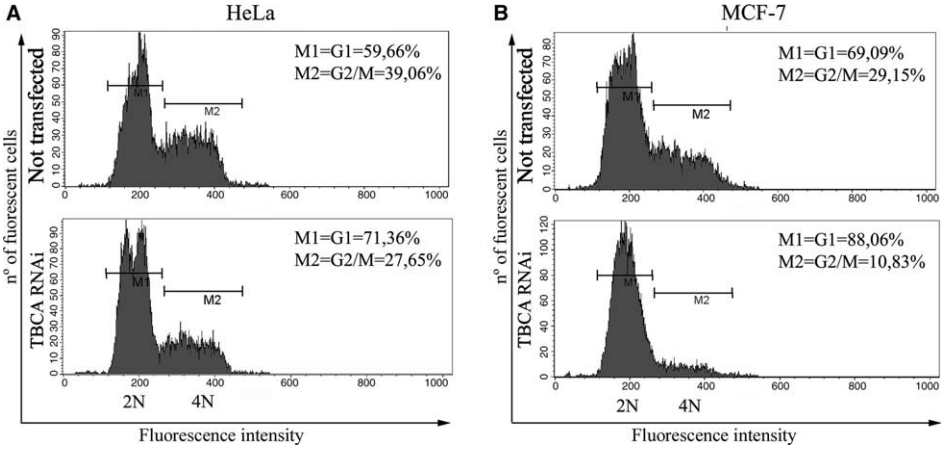

Fig. 6. TBCA knockdown by RNAi in HeLa and MCF-7 cells induces a G1 cell cycle arrest. DNA content of HeLa (A) and MCF-7 (B) cells not transfected and transfected with TBCA siRNA after 24 and 72 h, respectively, was analyzed by flow cytometry (FACS analysis). FACS profiles from one of two independent experiments show G1 cell cycle arrest. In each case, 30 000 cells were analysed. Cells transfected with non-target siRNA could not be stained with propidium iodide and analysed by FACS due to emission wavelength incompatibility.

nied also by a decrease of steady-state levels of α-tubulin. These results suggest that the ratio between α- and β-tubulin is strictly regulated in mammalian cells probably through their folding pathways. In HeLa cells, the alterations observed for Mt cytoskeleton may be responsible for changes in the actin cytoskeleton leading to the blebbing phenotype. Interestingly, the detected Mt alterations resemble those observed in plant and yeast TBCA mutants [10,12,16,17]. However, the phenotype in *Arabidopsis kis*$^{(A)}$ mutants did not show defects in actin cytoskeleton [16]. In MCF-7 cell line, slight changes in Mt cytoskeleton were detected at 48 h post-transfection when the TBCA protein steady-state levels start to decrease. However, this decrease was not reflected on α- and β-tubulin steady-state amounts until 96 h after transfection when cells go through dramatic cell shape alterations, like differentiation, and initiate to die. In spite of the differences between the two cell lines, our results indicate that the decrease in soluble tubulin amount, as a consequence of TBCA silence, correlates with cell death. In both cell lines death is preceded by a G1 cell cycle arrest that is probably due to the alterations of the Mt cytoskeleton. There are evidences that the destruction of the Mt cytoskeleton in interphase cells by itself is sufficient to induce G1 cell cycle arrest [32], which has been also closely related with differentiation in a variety of distinct mammalian cell types [33,34]. The differences found between HeLa and MCF-7 cell lines may be due to distinct intrinsic features and/or to the expression of distinct β-tubulin isotypes with different sensitivities to the absence of TBCA in these two cell lines.

TBCA silencing in both HeLa and MCF-7 cells induces a decrease in steady-state levels of procaspase-7 indicating an activation of caspase-7, one of the major effectors of apoptotic death signals [35]. Furthermore, the TBCA knockdown in HeLa cell line in the presence of the caspase activity inhibitor (Z-VAD-FMK) caused a delay in cell death and a decrease in PARP protein cleavage. These results strongly suggest the involvement of caspase activities in cell death caused by TBCA silence. However, in both cell lines, Anexin-V and PI staining indicated that cell death occurs essentially by necrosis/late apoptosis. A link between apoptosis and necrosis was already established in neurons where caspase inhibitors could reduce necrosis [31].

In conclusion, our results clearly show that TBCA is essential for cell viability in mammalian cells. Even so it is still not clear how TBCA knockdown affects Mt cytoskeleton, but probably this is a consequence of a decrease in the pool of α/β-tubulin heterodimers competent to polymerize.

Acknowledgements: We are deeply grateful to Dr. Sukalyan Chatterjee and Dr. Luís Viseu-Melo for critical reviewing and providing valuable suggestions about the manuscript, as well as to our colleagues Cecília Seixas and Joana Monteiro. We also thank Nuno Moreno for technical assistance in fluorescence microscopy and Mario Grãos and Margarida Santos for helping with flow cytometry analysis. S.N. received a fellowship from FCT (SFRH/BD/910/2000), Portugal and J.B. a fellowship associated to Grant BMC2001-0618 from the MEC, Spain.

References

[1] Downing, K.H. and Nogales, E. (1998) Tubulin and microtubule structure. Curr. Opin. Cell Biol. 10, 16–22.
[2] Joshi, H.C. (1998) Microtubule dynamics in living cells. Curr. Opin. Cell Biol. 10, 35–44.
[3] Hirokawa, N. (1994) Microtubule organization and dynamics dependent on microtubule-associated proteins. Curr. Opin. Cell Biol. 6, 74–81.
[4] Mandelkow, E. and Mandelkow, E.-M. (1995) Microtubules and microtubule associated proteins. Curr. Opin. Cell Biol. 7, 72–81.
[5] Lewis, S.A., Tian, G. and Cowan, N.J. (1997) The α- and β-tubulin folding pathways. Trends Cell Biol. 7, 479–484.
[6] Campo, R., Fontalba, A., Sánchez, L.M. and Zabala, J.C. (1994) A 14 kDa release factor is involved in GTP-dependent β-tubulin folding. FEBS Lett. 353, 162–166.
[7] Gao, Y., Melki, R., Walden, P.D., Lewis, S.A., Ampe, C., Rommelaere, H., Vandekerckhove, J. and Cowan, N.J. (1994) A novel cochaperonin that modulates the ATPase activity of cytoplasmic chaperonin. J. Cell Biol. 125, 989–996.
[8] Fontalba, A., Paciucci, R., Avila, J. and Zabala, J.C. (1993) Incorporation of tubulin subunits into dimers requires GTP hydrolysis. J. Cell Sci. 106, 627–632.
[9] Bhamidipati, A., Lewis, S.A. and Cowan, N.J. (2000) ADP ribosylation factor-like protein 2 (Arl2) regulates the interaction of tubulin-folding cofactor D with native tubulin. J. Cell Biol. 149, 1087–1096.
[10] Archer, J.E., Vega, L.R. and Solomon, F. (1995) Rbl2p, a yeast protein that binds to β-tubulin and participates in microtubule function in vivo. Cell 82, 425–434.
[11] Hoy, M.A., Macke, J.P., Roberts, B.T. and Geiser, J.R. (1997) *Saccharomyces cerevisiae PAC2* functions with *CIN1*, 2 and 4 in a pathway leading to normal microtubule stability. Genetics 146, 849–857.
[12] Radcliffe, P.A., Garcia, M.A. and Toda, T. (2000) The cofactor-dependent pathways for α- and β-tubulins in microtubule biogenesis are functionally different in fission yeast. Genetics 156, 93–103.
[13] Tian, G., Huang, Y., Rommelaere, H., Vandekerckhove, J., Ampe, C. and Cowan, N.J. (1996) Pathway leading to correctly folded β-tubulin. Cell 86, 287–296.
[14] Fanarraga, M.L., Avila, J., Guasch, A., Coll, M. and Zabala, J.C. (2001) Review: post-chaperonin tubulin folding cofactors and their role in microtubule dynamics. J. Struct. Biol. 135, 219–229.
[15] Fanarraga, M.L., Parraga, M., Aloria, K., del Mazo, J. and Zabala, J.C. (1999) Regulated expression of p14 (cofactor A) during spermatogenesis. Cell Motil. Cytoskel. 43, 243–254.
[16] Steinborn, K., Maulbetsch, C., Priester, B., Trautman, S., Pacher, T., Geiges, B., Kuttner, F., Lepiniec, L., Stierhof, Y. and Schwarz, H., et al. (2002) The *Arabidopsis PILZ* group genes encode tubulin-folding cofactor orthologs required for cell division but not cell growth. Genes Dev. 16, 959–971.
[17] Kirik, V., Grini, P.E., Mathur, J., Klinkhammer, I., Adler, K., Bechtold, N., Herzog, M., Bonneville, J.M. and Hulskamp, M. (2002) The *Arabidopsis* tubulin folding cofactor A gene is involved in the control of the α/β-tubulin monomer balance. Plant Cell 14, 2265–2276.
[18] Elbashir, S.M., Harborth, J., Weber, K. and Tuschl, T. (2002) Analysis of gene function in somatic mammalian cells using small interfering RNAs. Methods 26, 199–213.
[19] Meadus, W.J. (2003) A semi-quantitative RT-PCR method to measure the in vivo effect of dietary conjugated linoleic acid on porcine muscle PPAR gene expression. Biol. Proced. Online 5, 20–28.
[20] Schagger, H. and Jagow, G.V. (1987) Tricine–sodium dodecyl sulfate- polyacrylamide gel electroforesis for the separation of proteins in the range from 1 to 100 kDa. Anal. Biochem. 166, 368–379.
[21] Seixas, C., Casalou, C., Viseu Melo, L., Nolasco, S., Brogueira, A.P. and Soares, H. (2003) Subunits of the chaperonin CCT are associated with *Tetrahymena* microtubule structures and are involved in cilia biogenesis. Exp. Cell Res. 290, 303–321.
[22] Llosa, M., Aloria, K., Campo, R., Padilla, R., Avila, J., Sanchez-Pulido, L. and Zabala, J.C. (1996) The β-tubulin monomer release factor (p14) has homology with a region of the DnaJ protein. FEBS Lett. 397, 283–289.
[23] Harris, A.K. (1990) Protrusive activity of the cell surface and the movements of tissues cells in: Biomechanics of Active Movement and Division of Cells (Akkas, N., Ed.), NATO ASI Series, Vol. H42, pp. 249–290, Springer, Berlin.

[24] Cunningham, C.C. (1995) Actin polymerisation and intracellular solvent flow in cell surface blebbing. J. Cell Biol. 129, 1589–1599.
[25] Janmey, P.A., Cunningham, C.C., Oster, G.F. and Stossel, T.P. (1992) Cytoskeleton networks and osmotic pressure in relation to cell structure and motility in: Mechanics in Swelling: From Clay to Living Cells and Tissues (Karalis, Ed.), NATO ASI Series, Vol. H64, pp. 333–346, Springer, Berlin.
[26] Keller, H.U. and Zimmermann, A. (1986) Shape changes and chemokinesis of Walker 256 carcinosarcoma cells in response to colchicine, vinblastine, nocodazole and taxol. Invasion Metastasis 6, 33–43.
[27] Keller, H.U. and Eggli, P. (1998) Protrusive activity, cytoplasmic compartmentalization and restriction rings in locomoting blebbing Walker carcinosarcoma cells are related to detachment of cortical actin from the plasma membrane. Cell Motil. Cytoskel. 41, 181–193.
[28] Domnina, L.V., Ianova, O.Y., Pletjushkina, O.Y., Fetisova, E.K., Chernyak, B.V., Skulachev, V.P. and Vasiliev, J.M. (2004) Marginal blebbing during the early stages of TNF-induced apoptosis indicates alteration in actomyosin contractily. Cell Biol. Intern. 28, 471–475.
[29] Janicke, R.U., Sprengart, M.L., Wati, M.R. and Porter, A.G. (1998) Caspase-3 is required for DNA fragmentation and morphological changes associated with apoptosis. J. Biol. Chem. 273, 9357–9360.
[30] Los, M., Mozoluk, M., Ferrari, D., Stepczynska, A., Stroh, C., Renz, A., Herceg, Z., Wang, Z.-Q. and Schulze-Osthoff, K. (2002) Activation and caspase-mediated inhibition of PARP: a molecular switch between fibroblast necrosis and apoptosis in death receptor signaling. Mol. Biol. Cell 13, 978–988.
[31] Schwab, B.L., Guerini, D., Didszun, C., Bano, D., Ferrando-May, E., Fava, E., Tam, J., Xu, D., Xanthoudakis, S., Nicholson, D.W., Carafoli, E. and Nicotera, P. (2002) Cleavage of plasma membrane calcium pumps by caspases: a link between apoptosis and necrosis. Cell Death Differ. 9, 818–831.
[32] Sablina, A.A., Agapova, L.S., Chumakov, P.M. and Kopnin, B.P. (1999) p53 does not control the spindle assembly cell cycle checkpoint but mediates G1 arrest in response to disruption of microtubule system. Cell Biol. Int. 23, 323–334.
[33] DiCunto, F., Topley, G., Calautti, E., Hsiao, J., Ong, L., Seth, P.K. and Dotto, G.P. (1998) Inhibitory function of p21Cip1/WAF1 in differentiation of primary mouse keratinocytes independent of cell cycle control. Science 280, 1069–1072.
[34] Chang, B.D., Wuan, Y., Broude, E.V., Zhu, H., Schott, B., Fang, J. and Roninson, I.B. (1999) Role of p53 and p21waf1/cip1 in senescence-like terminal proliferation arrest induced in human tumor cells by chemotherapeutic drugs. Oncogene 18, 4808–4818.
[35] Earnshaw, W.C., Martins, L.M. and Kaufmann, S.H. (1999) Mammalian caspases: structure activation, substrates, and functions during apoptosis. Annu. Rev. Biochem. 68, 383–424.